Painlevé Integrability and N-Soliton Solution for the Whitham-Broer-Kaup Shallow Water Model Using Symbolic Computation

Cheng Zhang[a], Bo Tian[a,b,c], Xiang-Hua Meng[a], Xing Lü[a], Ke-Jie Cai[a], and Tao Geng[a]

[a] School of Science, Beijing University of Posts and Telecommunications, P. O. Box 122, Beijing 100876, China
[b] State Key Laboratory of Software Development Environment, Beijing University of Aeronautics and Astronautics, Beijing 100083, China
[c] Key Laboratory of Optical Communication and Lightwave Technologies, Ministry of Education, Beijing University of Posts and Telecommunications, Beijing 100876, China

Reprint requests to B. T.; E-mail: gaoyt@public.bta.net.cn

Z. Naturforsch. **63a,** 253 – 260 (2008); received December 21, 2007

With the help of symbolic computation, the Whitham-Broer-Kaup shallow water model is analyzed for its integrability through the Painlevé analysis. Then, by truncating the Painlevé expansion at the constant level term with two singular manifolds, the Hirota bilinear form is obtained and the corresponding N-soliton solution with graphic analysis is also given. Furthermore, a bilinear auto-Bäcklund transformation is constructed for the Whitham-Broer-Kaup model, from which a *one*-soliton solution is presented.

Key words: Whitham-Broer-Kaup Model; N-Soliton Solution; Auto-Bäcklund Transformation; Painlevé Analysis; Bilinear Form.

1. Introduction

In the last few decades, a large variety of physical, chemical and biological phenomena have been governed by nonlinear evolution equations (NLEEs) [1 – 4]. Much attention has been paid to find the exact analytical solutions of the NLEEs including soliton, periodic and rational solutions [1 – 5]. There has been a great development in various methods of finding the solutions [1 – 4], such as the inverse scattering transformation (IST) method [6, 7], the Bäcklund transformation (BT) [4, 8], the Darboux transformation [9], the Hirota bilinear method [10], the Painlevé method [11] and the algebra-geometric method [12]. Among these methods, the Hirota bilinear method is an important tool to deal with NLEEs and soliton problems, and it can be used to effectively construct the N-soliton solution in the form of an N-th-order polynomial in N exponentials for a large class of NLEEs [10]. One important step of this method is to transform the given NLEE into its bilinear form via suitable transformations. However, there is no universal method to find the transformations. In this paper, the authors report that one can generally obtain a dependent variable transformation which can transform a NLEE into its bilinear form by truncating the Painlevé expansion at the constant level term with one (two) singular manifold(s). Subsequently, further study can be continued via the Hirota bilinear method. For instance, the N-soliton solution can be obtained and the auto-BT in bilinear form can be constructed. For illustration, we consider the Whitham-Broer-Kaup (WBK) model [13]

$$\begin{cases} u_t + uu_x + v_x + qu_{xx} = 0, \\ v_t + (uv)_x + pu_{xxx} - qv_{xx} = 0, \end{cases} \tag{1}$$

where $u = u(x,t)$ is the field of a horizontal velocity and $v = v(x,t)$ the amplitude describing the deviation from the equilibrium position of the liquid; p and q are constants that represent different diffusion strengths. If $p = 0$ and $q \neq 0$, system (1) reduces to the classical long-wave equations that describe shallow water waves with diffusion [14]. If $p = 1$ and $q = 0$, system (1) becomes the variant Boussinesq equation [6]. In recent years, many efforts have been dedicated to the study of WBK equations, especially of their symmetries and conservation laws [14], their Bäcklund transformation [15] and rich families of exact analytical solutions by various effective methods [16]. It is specially mentioned that some new solitary wave structures have been revealed by the extended tanh-function method in [5]. However, to our knowledge, little research work has been done on this model by the Painlevé analysis and the Hirota bilinear method.

The structure of the present paper is arranged as follows: Section 2 gives a review of the well-known Painlevé analysis and applies this technique to the WBK model. In Section 3, by truncating the Painlevé expansion at the constant level term with two singular manifolds, we obtain the bilinear form for system (1) and give its N-soliton solution. Furthermore, Section 4 is devoted to the construction of an auto-BT in bilinear form for the WBK model. Finally, Section 5 is our conclusion and discussion.

2. Painlevé Analysis of the WBK Model

In this section, we give a brief review of the Painlevé analysis and illustrate each step by the coupled WBK model. As known, the Painlevé partial differential equation (PDE) analysis was first proposed by Weiss, Tabor and Carnevale (WTC) [17], which has been proved to be one of the most successful and widely applied tools in studying the integrability of PDEs. A given PDE is said to possess the Painlevé property [18] or be a Painlevé integrable model when it passes the Painlevé PDE analysis, i.e., the solutions of this PDE are "single-valued" in the neighbourhood of noncharacteristic, movable singular manifolds [6]. The Painlevé integrability is a necessary condition for being Lax- or IST-integrable [19]. Sequentially, by truncating the Painlevé expansion at the constant level term, one can obtain the associated BT, the Lax pair, the Darboux transformation [20], and so on.

According to the WTC procedure, the solutions of system (1) can be expanded in terms of the Laurent series as follows:

$$u(x,t) = \varphi^{-\alpha}(x,t)\sum_{j=0}^{\infty} u_j(x,t)\varphi^j(x,t), \tag{2}$$

$$v(x,t) = \varphi^{-\beta}(x,t)\sum_{j=0}^{\infty} v_j(x,t)\varphi^j(x,t), \tag{3}$$

where $\varphi(x,t) = 0$ is the equation of the singular manifold with α and β as positive integers to be determined. The algorithm of the Painlevé analysis for system (1) essentially consists of the following three steps:

Step a. Leading Order Analysis

The leading orders of the solutions of system (1) are assumed to be

$$u = u_0\varphi^{-\alpha}, \quad v = v_0\varphi^{-\beta}, \tag{4}$$

where u_0 and v_0 are analytical functions of (x,t). Substituting (4) into system (1) and balancing the highest-order derivative terms with the nonlinear terms, we obtain

$$\alpha = 1, \quad \beta = 2.$$

The leading coefficients u_0 and v_0 satisfy

$$-u_0^2 - 2v_0 + 2qu_0\varphi_x = 0, \tag{5}$$

$$-3u_0v_0 - 6qv_0\varphi_x - 6pu_0\varphi_x^2 = 0. \tag{6}$$

Solving (5) and (6) with respect to u_0 and v_0, we have: case 1:

$$u_0 = 2\sqrt{p+q^2}\varphi_x,\ v_0 = 2\left(-p-q^2+q\sqrt{p+q^2}\right)\varphi_x^2,$$

case 2:

$$u_0 = -2\sqrt{p+q^2}\varphi_x, v_0 = 2\left(-p-q^2-q\sqrt{p+q^2}\right)\varphi_x^2,$$

i. e., system (1) has two different expansion branches. In the following steps, we will show that system (1) possesses the Painlevé property in both expansion branches.

Step b. Finding the Resonances

This step in the Painlevé analysis is to find the resonances, i. e. the powers at which arbitrary coefficient functions appear in the series. Here we take case 1 as an example. We can apply the process analoguously to case 2. Substituting

$$\begin{aligned} u &= u_0\varphi^{-1} + u_j\varphi^{-1+j} \\ &= 2\sqrt{p+q^2}\varphi_x\varphi^{-1} + u_j\varphi^{-1+j}, \end{aligned} \tag{7}$$

$$\begin{aligned} v &= v_0\varphi^{-2} + v_j\varphi^{-2+j} \\ &= 2\left(-p-q^2+q\sqrt{p+q^2}\right)\varphi_x^2\varphi^{-2} + v_j\varphi^{-2+j} \end{aligned} \tag{8}$$

into system (1) and collecting the terms with the lowest powers of φ yields the general recursion relation

$$Q(j)\begin{pmatrix} u_j \\ v_j \end{pmatrix} = \begin{pmatrix} F_j \\ G_j \end{pmatrix}, \tag{9}$$

where

$$F_j = \Big(2q - 3jq + j^2q - 4\sqrt{p+q^2} + 2j\sqrt{p+q^2}\Big)\varphi_x^2 u_j - (2-j)\varphi_x v_j, \tag{10}$$

$$G_j = \big(9jp - 6j^2p + j^3p + 6q^2 - 2jq^2 - 6q\sqrt{p+q^2} + 2jq\sqrt{p+q^3}\Big)\varphi_x^3 u_j - \Big(6q - 5jq + j^2q + 6\sqrt{p+q^2} - 2j\sqrt{p+q^2}\Big)\varphi_x^2 v_j. \tag{11}$$

The resonances are given by

$$\det Q(j) = -(j-4)(j-3)(j-2)(1+j)(p+q^2)\varphi_x^4 = 0, \quad \text{valid for } j \geq 1.$$

Therefore the resonances occur at $j = -1, 2, 3, 4$, and the resonance $j = -1$ is usually associated with the arbitrariness of the function $\varphi(x,t)$, which describes the singular hypersurface.

Step c. Verifying the Compatibility Conditions

With the help of symbolic computation we insert the truncated expansions

$$u = \varphi^{-1}\sum_{j=0}^{4} u_j\varphi^j, \quad v = \varphi^{-2}\sum_{j=0}^{4} v_j\varphi^j \tag{12}$$

into system (1), where the upper limit of the sums is the largest resonance, $j = 4$. For the resonances $j = 2$ and $j = 3$ it turns out that there is only one independent equation defining u_j and v_j which means that either of them is arbitrary. For $j = 4$, there are two linear equations defining u_4 and v_4, but the rank of the matrix of the coefficients is *one*, so u_4 or v_4 is arbitrary. Therefore, system (1) has solutions of the forms (2) and (3) with the required number of arbitrary functions and so passes the Painlevé analysis.

Simultaneously, we can obtain v_1 by solving the equations with the second lowest powers of φ:

For case 1: $\quad v_1 = 2\Big(p + q^2 - q\sqrt{p+q^2}\Big)\varphi_{xx},$

for case 2: $\quad v_1 = 2\Big(p + q^2 + q\sqrt{p+q^2}\Big)\varphi_{xx}.$

3. Bilinear Form and *N*-Soliton Solution for the WBK Model

By truncating the Painlevé expansion at the constant level term with two singular manifolds, φ and ψ, we obtain

$$u = \frac{u_0}{\varphi} + \frac{u_0'}{\psi} + u_1' = 2\sqrt{p+q^2}\left[\log\left(\frac{\varphi}{\psi}\right)\right]_x + u_1', \tag{13}$$

$$v = \frac{v_0}{\varphi^2} + \frac{v_1}{\varphi} + \frac{v_0'}{\psi^2} + \frac{v_1'}{\psi} + v_2' = 2(p+q^2)\left[\log(\psi\varphi)\right]_{xx} - 2q\sqrt{p+q^2}\left[\log\left(\frac{\varphi}{\psi}\right)\right]_{xx} + v_2', \tag{14}$$

where we have taken (u_0, v_0) for one expansion branch and (u_0', v_0') for the other.

Assuming $\varphi \leftrightarrow g$, $\psi \leftrightarrow f$, $u_1' = 0$ and $v_2' = 4c\sqrt{p+q^2}$ (c is an arbitrary constant) in (13) and (14), we get the following dependent variable transformation:

$$u = 2\sqrt{p+q^2}\left[\log\left(\frac{g}{f}\right)\right]_x, \tag{15a}$$

$$v = 2(p+q^2)\left[\log(fg)\right]_{xx} - 2q\sqrt{p+q^2}\left[\log\left(\frac{g}{f}\right)\right]_{xx} + 4c\sqrt{p+q^2}. \tag{15b}$$

Through transformations (15a) and (15b) system (1) becomes the bilinear form

$$\begin{cases} \Big(D_t + \sqrt{p+q^2}D_x^2\Big)\, g\cdot f = 0, \\ \Big(D_xD_t + \sqrt{p+q^2}D_x^3 + 4cD_x\Big)\, g\cdot f = 0, \end{cases} \tag{16}$$

where D_t, D_x, D_x^2, D_x^3 and D_xD_t are bilinear derivative operators [21] defined by

$$D_x^m D_t^n a\cdot b \equiv \left(\frac{\partial}{\partial x} - \frac{\partial}{\partial x'}\right)^m \left(\frac{\partial}{\partial t} - \frac{\partial}{\partial t'}\right)^n \cdot a(x,t)b(x',t')\Big|_{x'=x,t'=t}. \tag{17}$$

Hereby we can construct the *N*-soliton solution of system (1) based on (16) as follows:

$$g = \sum_{\mu=0,1} \exp\left[\sum_{i=1}^{N}\mu_i(\eta_i + \widehat{\theta}_i) + \sum_{i<j}^{(N)}\mu_i\mu_j\delta_{ij}\right], \tag{18}$$

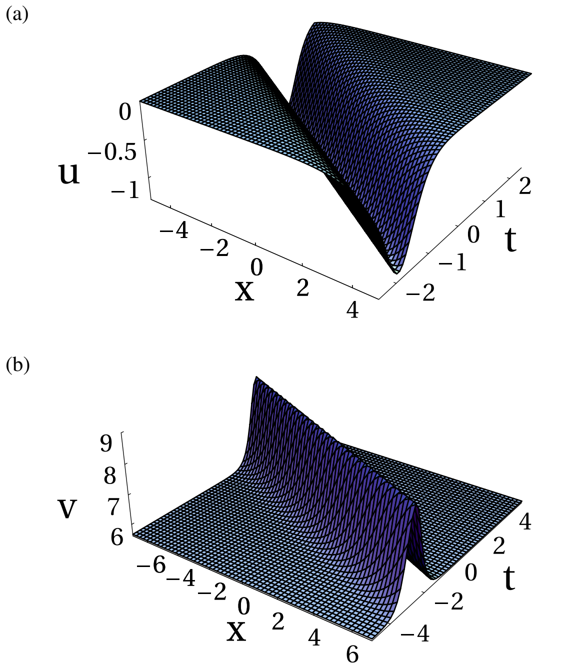

Fig. 1. (a) Evolution of an up-down bell-shaped soliton via (15a) together with expressions (23) – (26). The parameters are chosen as: $c = 1$, $p = 1$, $q = 1$, and $p_1 = 2$. (b) Evolution of a bell-shaped soliton via (15b) together with (23) – (26) by the same parameters as in (a).

$$f = \sum_{\mu=0,1} \exp\left[\sum_{i=1}^{N} \mu_i(\eta_i + \widehat{\theta_i'}) + \sum_{i<j}^{(N)} \mu_i\mu_j\delta_{ij}\right], \quad (19)$$

where

$$\eta_i = (p_i - q_i)(p + q^2)^{-\frac{1}{4}}x + (p_i^2 - q_i^2)t + \eta_i^0, \quad (20)$$

$$\exp\delta_{ij} = \frac{(p_i - p_j)(q_i - q_j)}{(p_i - q_j)(q_i - p_j)}, \quad (21)$$

$$\exp(\widehat{\theta_i}) = q_i, \quad \exp(\widehat{\theta_i'}) = p_i, \quad \text{and} \quad p_iq_i = c, \quad (22)$$

while p_i and q_i are parameters characterizing the i-th solition, η_i^0 $(i = 1, 2, \cdots, N)$ are arbitrary constants, $\sum_{\mu=0,1}$ is the summation over all possible combinations of $\mu_1 = 0, 1$, $\mu_2 = 0, 1, \cdots, \mu_N = 0, 1$, and $\sum_{i<j}^{(N)}$ is the summation over all possible pairs chosen from N elements under the condition $i < j$.

For $N = 1$, expressions (18) and (19) read

$$g = 1 + q_1\exp(\eta_1), \quad (23)$$

$$f = 1 + p_1\exp(\eta_1), \quad (24)$$

$$\eta_1 = (p_1 - q_1)(p + q^2)^{-\frac{1}{4}}x + (p_1^2 - q_1^2)t + \eta_1^0, \quad (25)$$

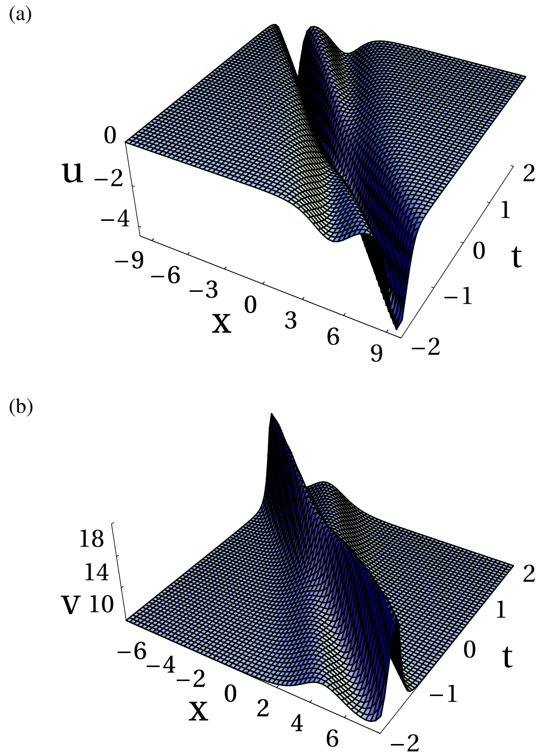

Fig. 2. (a) Elastic interaction of two solitons via (15a) together with expressions (27) – (31). The parameters are chosen as: $c = 1$, $p = 1$, $q = 1$, $p_1 = 3.5$, and $p_2 = 2$. (b) Elastic interaction of two solitons via (15b) together with (27) – (31) by the same parameters as in (a).

$$p_1q_1 = c, \quad (26)$$

which is a *one*-soliton solution of system (1).

For $N = 2$, expressions (18) and (19) can be written as

$$g = 1 + q_1\exp(\eta_1) + q_2\exp(\eta_2) + q_1q_2\frac{(p_1 - p_2)(q_1 - q_2)}{(p_1 - q_2)(q_1 - p_2)}\exp(\eta_1 + \eta_2), \quad (27)$$

$$f = 1 + p_1\exp(\eta_1) + p_2\exp(\eta_2) + p_1p_2\frac{(p_1 - p_2)(q_1 - q_2)}{(p_1 - q_2)(q_1 - p_2)}\exp(\eta_1 + \eta_2), \quad (28)$$

$$\eta_1 = (p_1 - q_1)(p + q^2)^{-\frac{1}{4}}x + (p_1^2 - q_1^2)t + \eta_1^0, \quad (29)$$

$$\eta_2 = (p_2 - q_2)(p + q^2)^{-\frac{1}{4}}x + (p_2^2 - q_2^2)t + \eta_2^0, \quad (30)$$

$$p_1q_1 = c, \quad p_2q_2 = c, \quad (31)$$

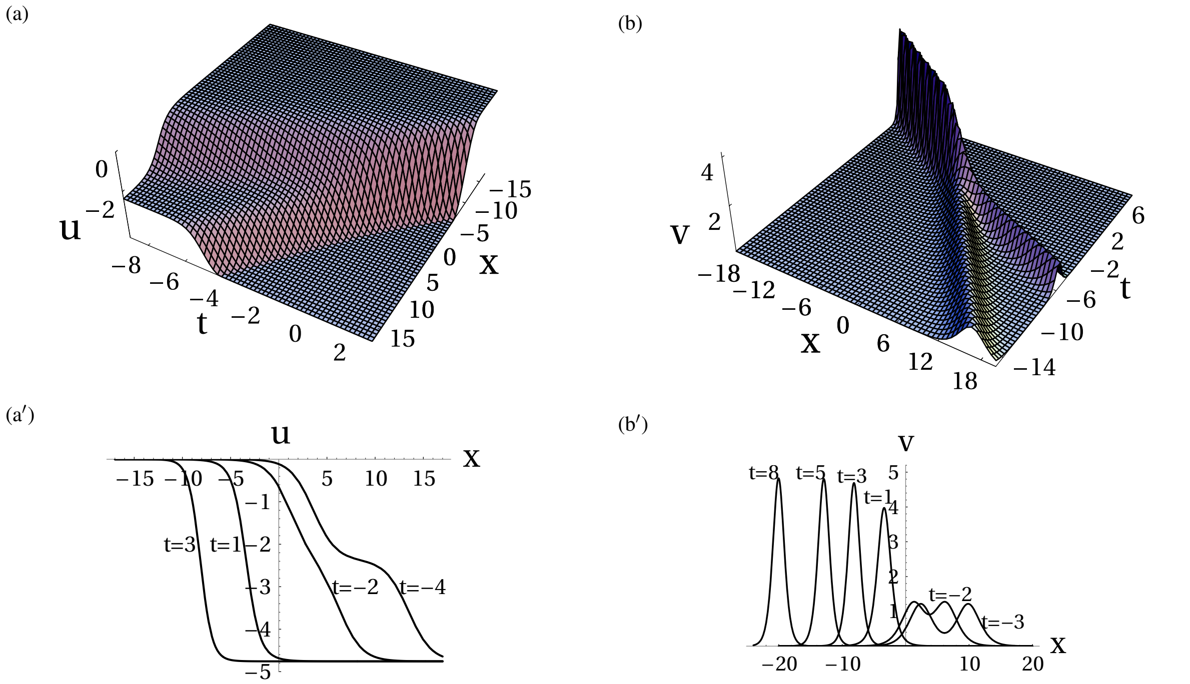

Fig. 3. (a) Surface of a *two*-shock-wave solution via (15a) together with expressions (27) – (31). The parameters are chosen as: $c = 0$, $p = 1$, $q = 1$, $p_1 = 2$, and $p_2 = 1$. (a') The corresponding trajectories of (a) at: $t = -4$, $t = -2$, $t = 1$, and $t = 3$. (b) Coalescence interaction of a *two*-soliton solution via (15b) together with (27) – (31) by the same parameters as in (a). (b') The corresponding trajectories of (b) at: $t = -3$, $t = -2$, $t = 1$, $t = 3$, $t = 5$, and $t = 8$.

which describe the *two*-soliton solution for the WBK model with appropriate parameters.

In order to better understand the mechanism of the WBK model, we draw some figures to analyze the behaviours of the solitons described by expressions (23) – (31). Figures 1a and 1b display two different bell-shaped soliton structures. In Figs. 2a and 2b, it is clearly seen that two solitons maintain their original amplitudes and velocities after collision except for the phase shifts. Additionally, by choosing different parameters in expressions (27) – (31), we can obtain other *two*-soliton interaction modes. For the special case $c = 0$, expressions (27) – (31) could describe the coalescence phenomenon of two travelling waves [22]. Figure 3a shows that two traveling waves which are both shock profiles coalesce into one large shock wave as the time increases, while Fig. 3b presents the coalescence interaction of two bell-shaped solitary waves. Figures 3a′ and 3b′, respectively, give specific views of Figs. 3a and 3b at different times. Actually, it turns out that a large-amplitude wave can be generated in Figure 3b.

We note that (21) can be expressed in different forms as

$$\exp\delta_{ij} = \frac{c(p_i - p_j)^2}{(c - p_i p_j)} \quad \text{or} \quad \exp\delta_{ij} = \frac{(c - p_i q_j)^2}{c(p_i - q_j)^2} \quad (i < j), \tag{32}$$

which may diverge when we take $c = 0$. Here, the arbitrary constant c enriches the solutions (18) and (19) by a long way and plays an important role in manipulating the interactions of solitons. The coefficients of the interaction terms in (27) and (28) vanish with $c = 0$, which leads to the coalescence phenomena. For $N \geq 3$, analogous results can be obtained by choosing appropriate p_i and q_i with the constraint $p_i q_i = 0$. In this sense, the solutions (18) and (19) obtained in this paper are more general and abundant. Moreover, with suitable choices of the parameters, the solutions reflect various soliton surfaces and can so be used to describe many more realistic phenomena in shallow water waves.

We know that p and q represent different diffusion strengths in system (1) and the widths of solitons vary with the changes of the parameters p and q. As seen

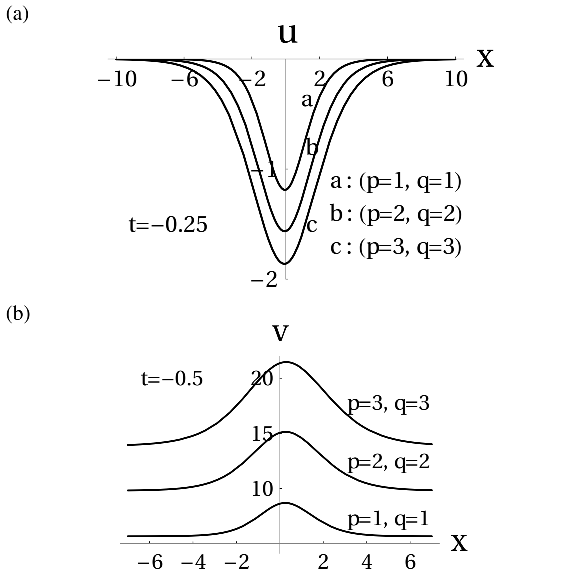

Fig. 4. (a) Three different choices of p and q with the same other parameters as in Fig. 1a via (15a) together with expressions (23) – (26) at $t = -0.25$. (b) Three different choices of p and q with the same other parameters as in Fig. 1a via (15b) together with (23) – (26) at $t = -0.5$.

in Figs. 4a and 4b, the widths of solitons get broaden while the values of p and q increase (and vice versa).

4. Auto-Bäcklund Transformation in Bilinear Form for the WBK Model

It is known that the auto-BT can give a hierarchy of explicit solutions including the N-soliton solution. In this section, based on (16), a bilinear auto-BT for system (1) is presented as

$$\left(D_t + \sqrt{p+q^2} D_x^2 + \delta\right) g \cdot g' = 0\,, \qquad (33a)$$

$$\left(D_t + \sqrt{p+q^2} D_x^2 + \delta\right) f \cdot f' = 0\,, \qquad (33b)$$

$$D_x f \cdot g' = \lambda g f'\,, \qquad (33c)$$

$$\left(D_x D_t + \sqrt{p+q^2} D_x^3 + 4cD_x\right) g \cdot g' = 0\,, \qquad (33d)$$

$$\left(D_x D_t + \sqrt{p+q^2} D_x^3 + 4cD_x\right) f \cdot f' = 0\,, \qquad (33e)$$

$$D_t f \cdot g' - 3\lambda \sqrt{p+q^2} D_x g \cdot f' - \mu g f' = 0\,, \qquad (33f)$$

where (g, f) and $\left(g', f'\right)$ are two different solutions of (16), and δ, λ, μ, and c are all arbitrary constants.

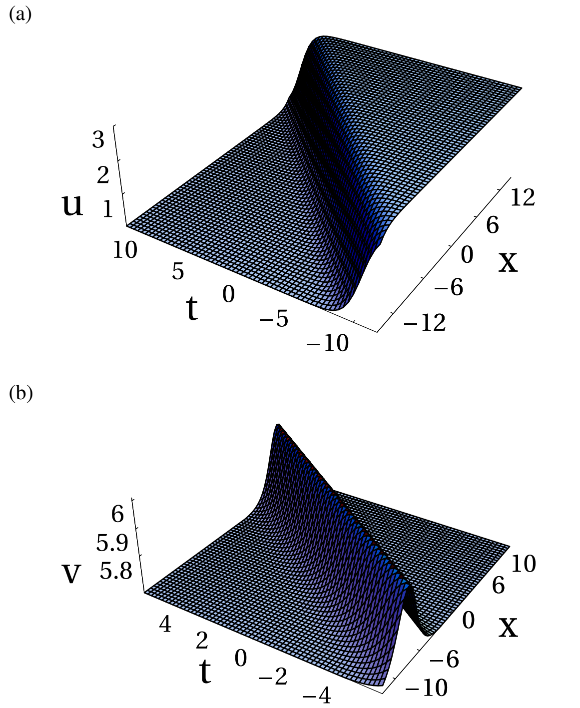

Fig. 5. (a) Stable propagation of a kink-shaped soliton via expression (37) with: $c = 1$, $k = 1$, $A = 1$, $p = 1$, and $q = 1$. (b) Stable propagation of a bell-shaped soliton via expression (38) with the same parameters as in (a).

For illustration, we can calculate the *one*-soliton solution from the seed solutions $g' = 1$ and $f' = 1$. Substituting the seed solutions into (33) yields

$$g_t + \sqrt{p+q^2} g_{xx} + \delta g = 0\,, \qquad (34a)$$

$$f_t + \sqrt{p+q^2} f_{xx} + \delta f = 0\,, \qquad (34b)$$

$$f_x = \lambda g\,, \qquad (34c)$$

$$g_{xt} + \sqrt{p+q^2} g_{xxx} + 4c g_x = 0\,, \qquad (34d)$$

$$f_{xt} + \sqrt{p+q^2} f_{xxx} + 4c f_x = 0\,, \qquad (34e)$$

$$f_t - 3\lambda \sqrt{p+q^2} g_x - \mu g = 0\,, \qquad (34f)$$

from which we can obtain

$$f = 1\,, \qquad (35)$$

$$g = 1 + A e^{kx - k^2 \sqrt{p+q^2} t}\,, \qquad (36)$$

where A and k are both arbitrary constants, and δ, λ, c, and μ are assumed to be zero.

Moreover, according to (15a), (15b), (35), and (36), the *one*-soliton solution of system (1) in explicit form can be expressed as

$$u = \frac{2Ak\sqrt{p+q^2}\mathrm{e}^{kx}}{\mathrm{e}^{k^2\sqrt{p+q^2}t} + A\mathrm{e}^{kx}}, \quad (37)$$

$$v = 4c\sqrt{p+q^2} + \frac{2Ak^2\left[p+q(q-\sqrt{p+q^2})\right]\mathrm{e}^{kx+k^2\sqrt{p+q^2}t}}{\left(\mathrm{e}^{k^2\sqrt{p+q^2}t} + A\mathrm{e}^{kx}\right)^2}. \quad (38)$$

It is found that the solutions (37) and (38) have kink and bell profiles which might be seen from Figs. 5a and 5b, respectively.

5. Conclusion and Discussion

In this paper, we have applied the Painlevé analysis to the WBK shallow water model and proved that this model possesses the Painlevé property in two different expansion branches. By truncating the Painlevé expansion at the constant level term with two singular manifolds, we have derived the dependent variable transformations which transform the WBK model into its bilinear form. Accordingly, the N-soliton solution for the WBK model has been presented and the interaction of solitons has been graphically illustrated and analyzed with different suitable choices of parameters. The behaviour of the solutions as functions of the chosen parameters has been discussed in Section 3. Furthermore, we have also constructed a bilinear auto-BT and obtained a *one*-solion solution from the seed solution. Based on the above results, it has been shown that the Painlevé analysis and the Hirota bilinear method can be used to study the WBK model.

The method with which we got the dependent variable transformations in Section 3 is applicable to a large class of NLEEs, such as the Korteweg-de Vries (KdV) equation, the coupled KdV equations, the nonlinear Schrödinger equation and the $(2+1)$-dimensional potential Kadomtsev-Petviashvili (pKP) equation [23]. Even for some nonintegrable NLEEs in the sense of not possessing the Painlevé property, such as the $(2+1)$-dimensional Boussinesq equation, the $(3+1)$-dimensional KP equation and the $(2+1)$-dimensional Jimbo-Miwa equation [24], the truncated Painlevé expansion can also be used to construct the dependent variable transformations. However, not for all NLEEs one can obtain the dependent variable transformations by this method. Examples are the nonisospectral sine-Gordon equation, the Nizhnik-Novikov-Veselov equation, the coupled Ramani equation [25] and the $(2+1)$-dimensional Dougherty-Krieger equation. So further studies on the relation between the Hirota bilinear method and the Painlevé analysis are worthwhile.

Acknowledgements

We express our sincere thanks to Prof. Y. T. Gao, Ms. J. Li, Ms. L. L. Li, Ms. H. Zhang, Mr. T. Xu, and Mr. H. Q. Zhang for their valuable comments. This work has been supported by the National Natural Science Foundation of China under Grant Nos. 60772023 and 60372095, by the Key Project of Chinese Ministry of Education (No. 106033), by the Open Fund of the State Key Laboratory of Software Development Environment under Grant No. SKLSDE-07-001, Beijing University of Aeronautics and Astronautics, by the National Basic Research Program of China (973 Program) under Grant No. 2005CB321901, and by the Specialized Research Fund for the Doctoral Program of Higher Education (No. 20060006024), Chinese Ministry of Education.

[1] R. K. Bullough and P. J. Caudrey (Eds.), Solitons, Springer, Berlin 1980.

[2] M. P. Barnett, J. F. Capitani, J. Von Zur Gathen, and J. Gerhard, Int. J. Quant. Chem. **100**, 80 (2004); F. D. Xie and X. S. Gao, Comm. Theor. Phys. **41**, 353 (2004); B. Tian and Y. T. Gao, Phys. Plasmas **12**, 054701 (2005); Phys. Lett. A **340**, 243, 449 (2005); **342**, 228 (2005); **359**, 241 (2006); **362**, 283 (2007); B. Tian, Y. T. Gao, and H. W. Zhu, Phys. Lett. A **366**, 223 (2007).

[3] G. Das and J. Sarma, Phys. Plasmas **6**, 4394 (1999); Z. Y. Yan and H. Q. Zhang, J. Phys. A **34**, 1785 (2001); W. P. Hong, Phys. Lett. A **361**, 520 (2007); Y. T. Gao and B. Tian, Phys. Plasmas **13**, 112901 (2006); Phys. Plasmas Lett. **13**, 120703 (2006); Phys. Lett. A **349**, 314 (2006); B. Tian, W. R. Shan, C. Y. Zhang, G. M. Wei, and Y. T. Gao, Eur. Phys. J. B (Rapid Not.) **47**, 329 (2005); B. Tian, G. M. Wei, C. Y. Zhang, W. R. Shan, and Y. T. Gao, Phys. Lett. A **356**, 8 (2006).

[4] B. Tian and Y. T. Gao, Phys. Plasmas Lett. **12**, 070703

(2005); Eur. Phys. J. D **33**, 59 (2005); Y. T. Gao and B. Tian, Phys. Lett. A **361**, 523 (2007); Eur. Phys. Lett. **77**, 15001 (2007).

[5] T. Xu, J. Li, H. Q. Zhang, Y. X. Zhang, Z. Z. Yao, and B. Tian, Phys. Lett. A **369**, 458 (2007).

[6] M. J. Ablowitz and P. A. Clarkson, Soliton, Nonlinear Evolution Equations and Inverse Scattering, Cambridge University Press, New York 1991.

[7] M. Wadati, K. Konno, and Y. H. Ichikawa, J. Phys. Soc. Jpn. **53**, 2642 (1983).

[8] M. Wadati, J. Phys. Soc. Jpn. **38**, 673 (1975); M. Wadati, H. Sanuki, and K. Konno, Prog. Theor. Phys. **53**, 419 (1975); K. Konno and M. Wadati, Prog. Theor. Phys. **53**, 1652 (1975).

[9] V. B. Matveev and M. A. Salle, Darboux Transformation and Soliton, Springer, Berlin 1991; V. G. Dubrousky and B. G. Konopelchenko, J. Phys. A **27**, 4619 (1994).

[10] R. Hirota, in: Direct Method in Soliton Theory (Eds. R. K. Bullough and P. S. Caudrey), Springer, Berlin 1980.

[11] F. Caruello and M. Tabor, Physica D **39**, 77 (1989).

[12] E. D. Belokolos, A. I. Bobenko, V. Z. Enol'skii, A. R. Its, and V. B. Matveev, Algebra-Geometrical Approach to Nonlinear Integrable Equations, Springer-Verlag, Berlin 1994; D. P. Novikov, J. Math. **40**, 136 (1999); C. W. Cao, X. G. Geng, and H. Y. Wang, J. Math. Phys. **43**, 621 (2002).

[13] G. B. Whitham, Proc. R. Soc. A **299**, 6 (1967); L. J. Broer, Appl. Sci. Res. **31**, 377 (1975); D. J. Kaup, Prog. Theor. Phys. **54**, 369 (1975).

[14] B. A. Kupershmidt, Commun. Math. Phys. **99**, 51 (1985).

[15] E. G. Fan and H. Q. Zhang, Appl. Math. Mech. **19**, 667 (1998).

[16] Z. Y. Yan and H. Q. Zhang, Phys. Lett. A **285**, 355 (2001); F. D. Xie, Z. Y. Yan, and H. Q. Zhang, Phys. Lett. A **285**, 76 (2001); Y. Chen and Y. Zheng, Int. J. Mod. Phys. C **14**, 601 (2003); Y. Chen, Q. Wang, and B. Li, Chaos, Solitons and Fractals **22**, 675 (2004); Y. Chen and Q. Wang, Phys. Lett. A **347**, 215 (2005).

[17] J. Weiss, M. Tabor, and G. Carnevale, J. Math. Phys. **24**, 522 (1983).

[18] R. Conte (Ed.), The Painlevé Property, One Century Later, Springer, NewYork 1999.

[19] S. L. Zhang, B. Wu, and S. Y. Lou, Phys. Lett. A **300**, 40 (2002); A. Bekir, Chaos, Solitons and Fractals **32**, 449 (2007).

[20] P. G. Estévez, Inverse Problems **17**, 1043 (2001).

[21] R. Hirota, Phys. Rev. Lett. **27**, 1192 (1971); R. Hirota and J. Satsumam, J. Phys. Soc. Jpn. **40**, 611 (1978); R. Hirota, X. B. Hu, and X. Y. Tang, J. Math. Anal. Appl. **288**, 326 (2003).

[22] T. Xu, C. Y. Zhang, J. Li, H. Q. Zhang, L. L. Li, and B. Tian, Z. Naturforsch. **61a**, 652 (2006); T. Xu, C. Y. Zhang, J. Li, X. H. Meng, H. W. Zhu, and B. Tian, Wave Motion **44**, 262 (2007).

[23] T. Alagesan, Y. Chung, and K. Nakkeeran, Chaos, Solitons and Fractals **26**, 1203 (2005).

[24] G. Q. Xu, Chaos, Solitons and Fractals **30**, 71 (2006).

[25] X. B. Hu and D. L. Wang, Appl. Math. Lett. **13**, 45 (2000).